



# A new time integration scheme for Cahn-Hilliard equations

R. Schaefer<sup>1</sup>, M. Smółka<sup>1</sup>, L. Dalcin<sup>2</sup>, and M. Paszyński<sup>1</sup>

<sup>1</sup> AGH University of Science and Technology, Krakow, Poland

<sup>2</sup> King Abdullah University of Science and Technology, Thuwal, Saudi Arabia

## Abstract

In this paper we present a new integration scheme that can be applied to solving difficult non-stationary non-linear problems. It is obtained by a successive linearization of the Crank-Nicolson scheme, that is unconditionally stable, but requires solving non-linear equation at each time step. We applied our linearized scheme for the time integration of the challenging Cahn-Hilliard equation, modeling the phase separation in fluids. At each time step the resulting variational equation is solved using higher-order isogeometric finite element method, with B-spline basis functions. The method was implemented in the PETIGA framework interfaced via the PETSc toolkit. The GMRES iterative solver was utilized for the solution of a resulting linear system at every time step. We also apply a simple adaptivity rule, which increases the time step size when the number of GMRES iterations is lower than 30. We compared our method with a non-linear, two stage predictor-multicorrector scheme, utilizing a sophisticated step length adaptivity. We controlled the stability of our simulations by monitoring the Ginzburg-Landau free energy functional. The proposed integration scheme outperforms the two-stage competitor in terms of the execution time, at the same time having a similar evolution of the free energy functional.

*Keywords:* isogeometric analysis, Cahn-Hilliard equations, non-stationary problems, GMRES solver

## 1 Introduction

Cahn-Hilliard equations [8, 9] can be used in modeling the separation of the two phases of a fluid, as well as for the cancer growth modeling [12].

The Cahn-Hilliard equations pose a challenging computational problem, therefore their time integration requires unconditionally stable schemes and appropriate time step adaptation procedures. The standard approach requires numerical solution of the non-linear algebraic equation at every time step, compare [9]. The strong form of the Cahn-Hilliard equation has fourth order with respect to the space variables, and thus, when solving their weak form in the space domain by Finite Element Method (FEM), the isogeometric B-splines of at least second order should be used as a basis [7]. Such functions are  $C^1$  at the interfaces between elements and  $C^\infty$  inside them [9]. Both mentioned computational challenges make the numerical solution of the Cahn-Hilliard equation difficult and time consuming.

We propose a linearized, mixed Finite Difference/Finite Element scheme for solving initial-boundary value problem for the Cahn-Hilliard equations. In the space domain the solution is approximated by means of higher order isogeometric finite element method with B-spline basis. The linearized version of the Crank-Nicolson integration scheme, that is unconditionally stable, is utilized for the time integration.

Our non-stationary solver has been implemented in the PETIGA toolkit [6] supporting the isogeometric computations. The PETIGA itself is a part of the PETSc toolkit [1, 2, 3]. For the solution of the linear problem at every time step, we use the GMRES procedure available from the PETSc library.

We also use a simple adaptation scheme, that increases the time step size each time the number of iterations of the GMRES solver is lower than 30. The performed simulations show the advantage of our linearized scheme over a sophisticated two-stage predictor-multicorrector non-linear time-adaptive scheme from [9].

## 2 Weak formulations of the Cahn-Hilliard equations

### 2.1 Strong formulation

This section presents the derivation of the weak form of Cahn-Hilliard equations based on [8]. Let us consider the following Cauchy problem.

Find  $u \in C^1(0, T; C^4(\Omega))$  such that

$$u_t = \nabla \cdot (B(u)\nabla (-\gamma\Delta u + \Psi'(u))) \quad \text{on } [0, T] \times \Omega \quad \text{and} \quad u(0, x) = u_0(x) \quad \text{on } \Omega, \quad (1)$$

where  $\Omega$  is an open subset of  $\mathbb{R}^n$  with smooth boundary and  $\gamma > 0$  is a constant.  $u$  is usually interpreted as the difference of the two fluid phase concentrations, hence  $u \in [-1, 1]$ . In such a case  $B(u) \geq 0$  is the diffusional mobility, whereas  $\Psi(u)$  is the homogeneous free energy. A crucial notion in the theory of Cahn-Hilliard equations is the Ginzburg-Landau free energy

$$\mathcal{E}(u) = \int_{\Omega} \left( \frac{\gamma}{2} |\nabla u|^2 + \Psi(u) \right) dx. \quad (2)$$

We introduce the following boundary conditions

$$\mathbf{n} \cdot (B(u)\nabla (-\gamma\Delta u + \Psi'(u))) = 0, \quad \mathbf{n} \cdot \nabla u = 0 \quad \text{on } [0, T] \times \partial\Omega, \quad (3)$$

where  $\mathbf{n}$  is the outer normal to  $\partial\Omega$ . Furthermore, we assume that the mobility functional  $B$  is of the following form

$$B(u) = (1 - u^2)^m \bar{B}(u)$$

where  $m \geq 1$  and  $\bar{B} : [-1, 1] \rightarrow \mathbb{R}$  is and  $C^1$ -regular, bilaterally bounded function,

$$0 < b_0 \leq \bar{B}(u) \leq B_0,$$

We also assume that the free energy functional  $\Psi$  might be decomposed into two parts

$$\Psi = \Psi_1 + \Psi_2,$$

where  $\Psi_2 \in C^2([-1, 1])$  and  $\Psi_1 : (-1, 1) \rightarrow \mathbb{R}$  is convex and satisfies

$$\Psi_1''(u) = (1 - u^2)^{-m} F(u)$$

for some positive function  $F$  of the class  $C^1([-1, 1])$ .

Finally, following [8], we select the functions  $B$  and  $\Psi$  as:

$$\begin{aligned} B(u) &= 1 - u^2, \\ \Psi(u) &= \frac{\theta}{2} ((1 + u) \log(1 + u) + (1 - u) \log(1 - u)) + 1 - u^2. \end{aligned} \tag{4}$$

### 2.2 Weak formulation $L^2$ in time

The following weak formulation is presented in [8] together with the respective existence theorem. We seek  $u \in L^2(0, T; H^2(\Omega)) \cap L^\infty(0, T; H^1(\Omega)) \cap C([0, T]; L^2(\Omega))$  such that  $u_t \in L^2(0, T; (H^1(\Omega))')$  and  $B(u)\nabla(-\gamma\Delta u + \Psi'(u)) \in L^2(\Omega_T; \mathbb{R}^n)$ , that satisfies (1) in the following sense

$$\int_0^T \langle u_t(t), \zeta(t) \rangle dt = - \int_{\Omega_T} [\gamma \nabla u \cdot (B(u)\nabla \zeta) + (B\Psi''(u)(u)\nabla u \cdot \nabla \zeta)] dx dt \tag{5}$$

for arbitrary  $\zeta \in L^2(0, T; H^1(\Omega))$  such that  $\nabla \zeta \in L^2(0, T; H^1(\Omega; \mathbb{R}^n)) \cap L^\infty(\Omega_T; \mathbb{R}^n)$  and  $\nabla \zeta \cdot \mathbf{n} = 0$ .

### 2.3 Weak formulation $C^1$ in time

Following [9] we introduce

$$U = \{u \in H^2(\Omega) \cap L^\infty(\Omega); \text{tr}(\nabla u \cdot \mathbf{n}) = 0\} \tag{6}$$

We define the space differential operator  $A : U \rightarrow U'$ , such that

$$\langle A(u), w \rangle = \int_{\Omega} [\gamma \nabla u \cdot (B(u)\nabla w) + (B\Psi''(u)(u)\nabla u \cdot \nabla w)] dx \tag{7}$$

and time-derivative operator  $\cdot_t : C^1(0, T; U) \rightarrow C(0, T; U')$  such that

$$\langle u_t(t), w \rangle = \int_{\Omega} \frac{\partial u}{\partial t}(t) \cdot w dx, \quad \forall t \in [0, T]. \tag{8}$$

Then we look for  $u \in C^1(0, T; U)$  such that

$$\langle u_t(t), w \rangle + \langle A(u(t)), w \rangle = 0 \quad \forall w \in U, \quad \forall t \in [0, T] \quad \text{and} \quad u(0, x) = u_0(x) \text{ a.e. on } \Omega. \tag{9}$$

### 2.4 Finite difference schemes for semicontinuous variational equation

We introduce the network  $\{t_0 = 0, t_1, \dots, t_K = T\} \subset [0, T]$ . To be coherent with the applied notation we introduce the simple "dualizing" operator  $\tau : U \rightarrow U'$  such that

$$\langle \tau(u), w \rangle = \int_{\Omega} u \cdot w, dx \quad \forall w \in U \tag{10}$$

Three finite difference schemes will be considered. The first is the forward Euler scheme:

$$\left\langle \tau \left( \frac{u^{i+1} - u^i}{t_{i+1} - t_i} \right), w \right\rangle + \langle A(u^i), w \rangle = 0 \quad \forall w \in U, \quad i = 1, \dots, K, \tag{11}$$

where  $u^0 \in U$  is the initial condition, and  $u^i = u(t_i)$ . The second scheme is the Crank-Nicolson method:

$$\left\langle \tau \left( \frac{u^{i+1} - u^i}{t_{i+1} - t_i} \right), w \right\rangle + \frac{1}{2} \langle (A(u^{i+1}) + A(u^i)), w \rangle = 0$$

$$\forall w \in U, \quad i = 1, \dots, K. \tag{12}$$

Finally, if  $A \in C^1(U)$  we can use a linearized three-level scheme

$$\left\langle \tau \left( \frac{u^{i+2} - u^i}{t_{i+2} - t_i} \right), w \right\rangle + \left\langle \left( \frac{1}{2} DA|_{u^{i+1}} (u^{i+2} + u^i - 2u^{i+1}) + A(u^{i+1}) \right), w \right\rangle = 0$$

$$\forall w \in U, \quad i = 1, \dots, K. \tag{13}$$

Its only disadvantage is that the double initial condition  $u^0, u^1 \in U$  has to be known. But this obstacle can be easily overcome by the single execution of a simpler non-linear scheme, like the Crank-Nicolson one, in order to obtain the additional initial condition  $u^1$ .

Each of these schemes (11, 12, 13) can be effectively computed if we replace the solutions  $u^i$  and the test function  $w$  by their approximations  $u_{h,p}^i, w \in V_{h,p}$  from the proper Finite Element space. In such a case equations (11, 12, 13) become mixed FD/FEM numerical schemes.

The Euler mixed scheme is very fast, because it does not need to solve any system of equations by progressing in time. However, its computational cost can be remarkable because of the necessary high time-step refinement (numerical instability). It can even become impossible to apply if the numerical stability cannot be achieved. The second, mixed Crank-Nicolson scheme is unconditionally stable, but needs to solve the algebraic non-linear system at each time step.

The linearized scheme (13) makes an advantageous compromise between the conditioning (unconditional stability) and computational cost. It needs to solve the linear system in each time step instead of a non-linear one. The detailed definition, the proof of convergence and numerical stability condition of (13) can be found in [16]. We also refer to [17] for a broader review of two- and three level mixed schemes for non-linear parabolic PDEs.

### 3 Numerical results

The numerical results presented in this section has been performed on a single node of ATARI Linux cluster at the Department of Computer Science, AGH University of Science and Technology. The node is equipped with 16 cores, 2.4 GHz clock and 16 GB of RAM.

#### 3.1 Cahn-Hilliard simulations

We performed numerical solution of the Cauchy problem (1) in the weak form,  $C^1$ -regular with respect to the time variable (9). The space domain of the solution is two dimensional  $\Omega = (0, 1)^2$ . We accepted the functions  $B$  and  $\Psi$  of the form (4), where  $\theta = 1.5$  is a dimensionless number which represents the ratio between the critical temperature  $\Xi_c$  (the temperature at which the two phases attain the same composition) and the absolute temperature  $\Xi$ ,  $\gamma = \frac{1}{N^2}$  where  $N$  is the mesh size in one direction with periodic boundary conditions and  $u_0(x) = 2\bar{c} - 1 + r$ , where  $\bar{c} = 0.63$  is the average concentration, while  $r$  is the scalar random perturbation with the uniform distribution  $\mathcal{U}(\Omega)$ .

Table 1: Comparison of linear scheme with simple time adaptation and non-linear schemes with advanced time adaptation.

		Linear scheme		Non-linear scheme	
N	p	iterations	time [s]	iterations	time [s]
$(64 + 2)^2$	2	250	29s	120	34s
$(128 + 2)^2$	2	250	102s	150	109s
$(256 + 2)^2$	2	256	498s	163	634s

In our simulations we utilize the GMRES solver for solution of the linear system at every time step. We define a simple time adaptation algorithm, that increases the time step each time the GMRES solver requires less than 30 iterations to converge. The same linear solver was used for solving a series of linear problems appearing in the Newton algorithm, by computing the additional initial condition from the Crank-Nicolson equations.

The snapshots from the Cahn-Hilliard simulations capturing phase separation process at different time steps are presented in Figure 1. The results concerns the case with  $N = 128^2$  and second order B-splines. For smaller mesh size, there are some problems with convergence of the free energy functional. The numerical experiments have been verified by monitoring the evolution of the Ginzburg-Landau free energy (2). The evolution of the energy is presented in Figure 2. We also provide in Figure 4 the history of time step evolution of our simple adaptation algorithm, based on monitoring the number of iterations of the GMRES solver.

### 3.2 Comparison with non-linear scheme

We have performed the comparison of our linearized scheme utilizing simple time step adaptation rule with a complex, non-linear scheme implemented in the PETIGA library (see [9]). The latter is a two-stage predictor-multicorrector algorithm based on the generalized- $\alpha$  method and equipped with a sophisticated time step adaptation strategy following the lines of the embedded Runge-Kutta methods. Three types of the B-spline spatial approximation were applied with the various numbers of degrees of freedom  $N = 64^2, 128^2, 256^2$  and the second order polynomials.

The evolution of the free Ginzburg-Landau energy (2) during simulation by using both schemes is presented in Figures 2, 3. Both simulations were stopped where they reached the assumed, identical level of free Ginzburg-Landau energy. The process of the phase separation is characterized by the constant decay of this energy towards an equilibrium state, so the maturity of this process can be assessed by the energy value observation. Stopping both methods after they reached the same value of the free Ginzburg-Landau energy allow us, in particular, to compare their computational cost of reaching the final state with a comparable accuracy.

The simulation results are summarized in Table 1. The time step evolution for both schemes is presented in Figures 4 and 5. The analysis of the results leads to the following conclusions.

- In general, the proposed linearized scheme with a simple time adaptation rule is faster than the reference one, which uses a sophisticated time step adaptation.
- The reference scheme performs generally much less time steps than the linearized one, until the simulations were stopped when the free energy reached the same assumed limit. The comparison of the wall execution time (see Table 1) shows that one step of the linearized scheme is approximately two times cheaper than a respective step of the reference scheme.

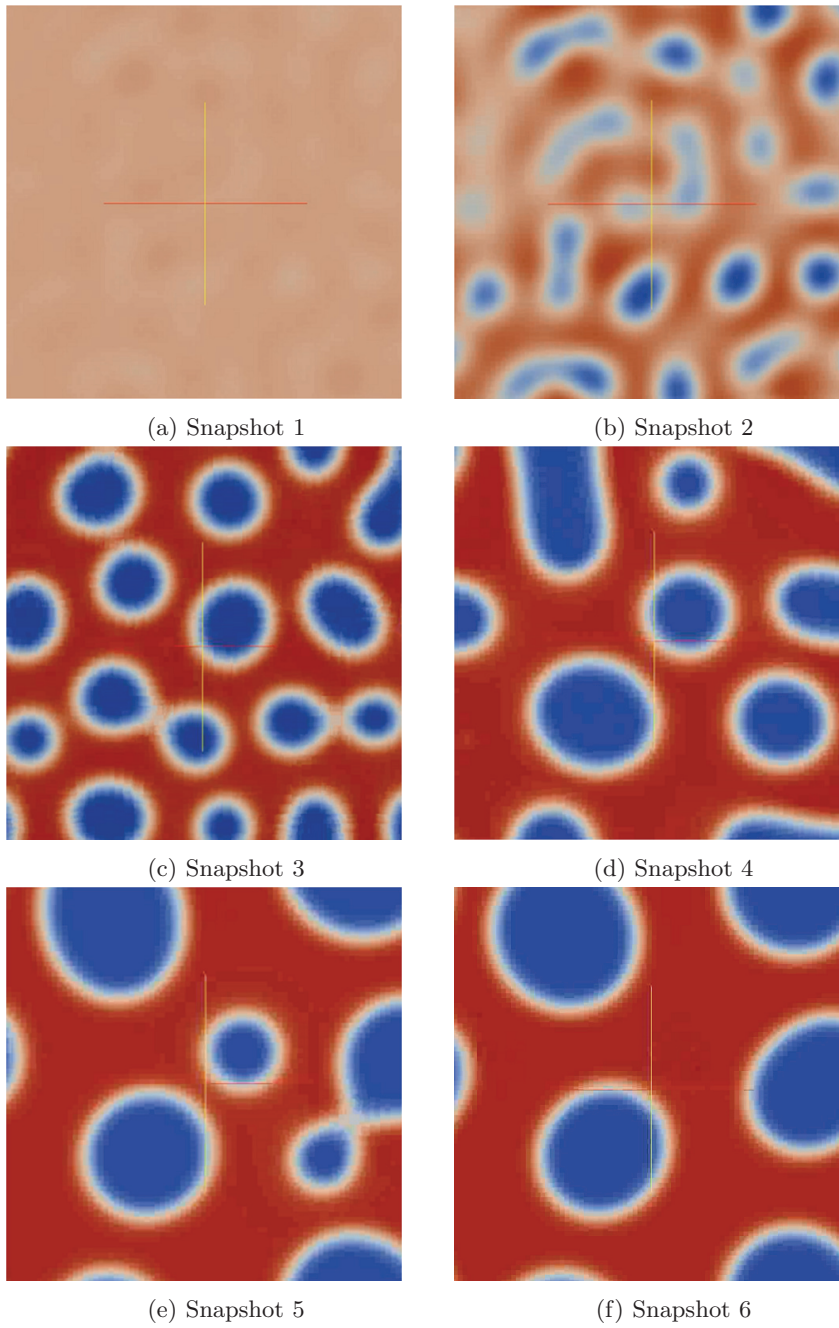


Figure 1: Snapshots from the Cahn-Hilliard simulation solution by using the linearized scheme.

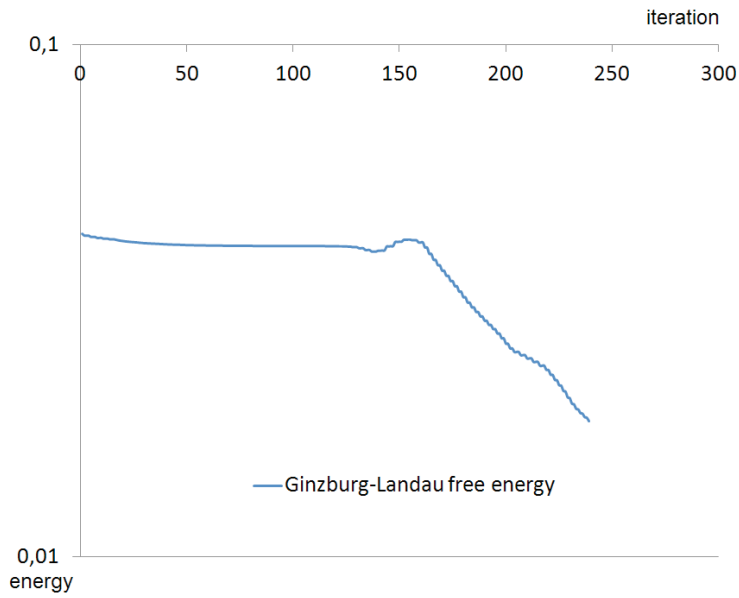


Figure 2: Evolution of the Ginzburg-Landau free energy for the linearized scheme.

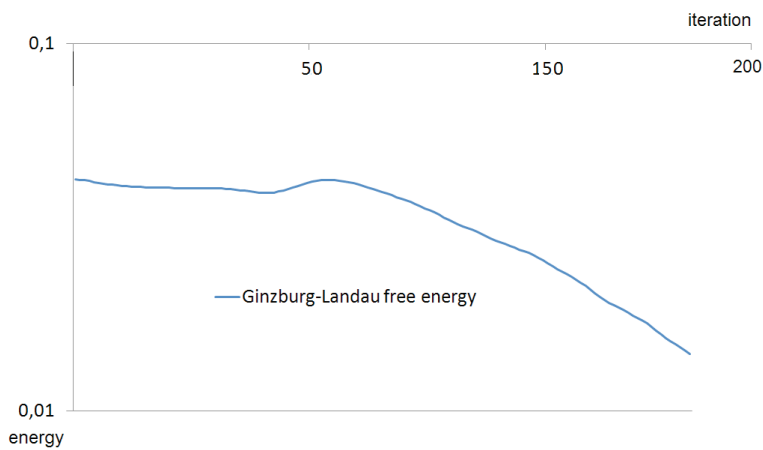


Figure 3: Evolution of the Ginzburg-Landau free energy for the non-linear scheme.

The computational cost discrepancy results from the weak numerical stability of the reference scheme and the necessity of the frequent expensive multicorrection and time step modification (see Figure 4).

- The general increasing trend of time step size is similar for both methods (see Figures 4, 5). However, it increases monotonically and smoothly in case of linearized scheme, whereas it strongly oscillates in case of the reference one, despite the sophisticated adaptation strategy applied. It shows that the proposed implicit scheme handles the strong nonlinearity appearing in the elliptic part of Cahn-Hilliard equations much better.

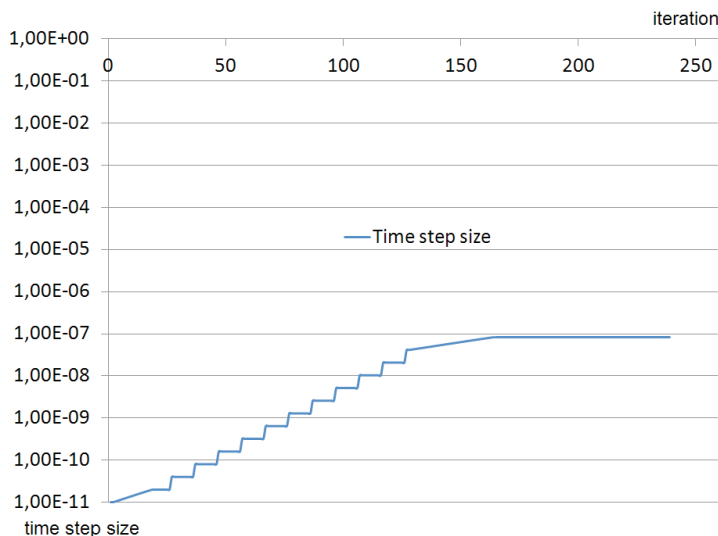


Figure 4: Time step evolution for the linearized scheme.

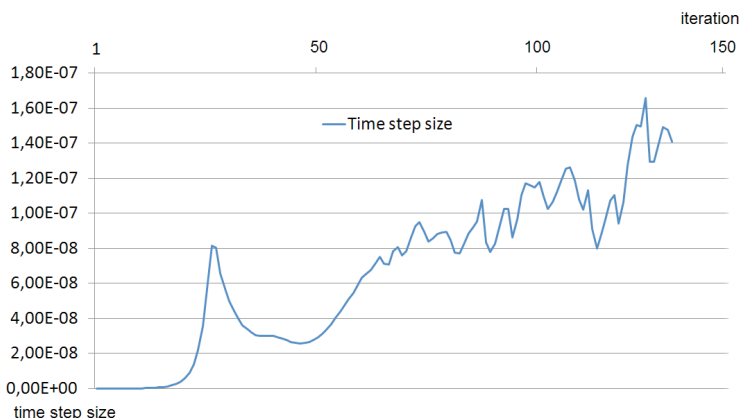


Figure 5: Time step evolution for the non-linear scheme.

- The speedup of linearized scheme with respect to the reference one grows when we increase the number of degrees of freedom in the spatial approximation of the solution (see Table 1). The linearized scheme would be then recommendable when the high accuracy of the solution is required.

## 4 Conclusions

In this paper we present a fast partial differential integration method for difficult non-stationary problems, based on the linearized version of the Crank-Nicolson scheme (13). The method is applied to the challenging non-linear Cahn-Hilliard parabolic equation. The mathematical background concerning strong, weak and semi-continuous formulations of the initial-boundary

value problems for Cahn-Hilliard equation is provided.

The integration scheme is implemented within the PETIGA framework, a part of the PETSc toolkit for isogeometric finite element method simulations. The GMRES solver has been used for solving the linear system at every time step. We have utilized a simple time adaptation scheme, where the time step length follows the number of iterations of the GMRES algorithm.

Mathematical considerations are followed by the results of numerical simulations, presenting the separation of two phases by means of the Cahn-Hilliard equations.

We compare the linearized scheme with a two stage predictor-multicorrector reference scheme, associated with a sophisticated time step adaptation (see [9]). We have shown that the linearized scheme with a simple time step adaptation outperforms the original method in terms of execution time. Moreover, it handles much better the strong nonlinearity appearing in the elliptic part of Cahn-Hilliard equations and is recommendable for the case in which the high accuracy of solution is required.

The future work may involve incorporating of multi-frontal, direct solver for the linear system solution and improving the time step adaptation. Moreover we plane to execute the whole system on a parallel distributed memory Linux cluster, using efficient isogeometric multi-frontal direct solvers [14, 11], as well as porting this algorithm to a GPU environment, using our fast GPU solver for linear algebraic systems [13].

The future work may also include speeding up the numerical integration of GPGPU [15, 4, 10] or incorporating multi-grid solvers [5].

## Acknowledgments

The work presented in this paper, in particular the visits of Lisandro Dalcin, PhD. at AGH has been supported by Polish National Science Center grant no. DEC-2012/07/B/ST6/01229.

## Bibliography

## References

- [1] S. Balay, S. Abhyankar, M. F. Adams, J. Brown, P. Brune, K. Buschelman, V. Eijkhout, W. D. Gropp, D. Kaushik, M. G. Knepley, L. Curfman McInnes, K. Rupp, B. F. Smith, H. Zhang, *PETSc Web Page*, <http://www.mcs.anl.gov/petsc> (2014)
- [2] S. Balay, S. Abhyankar, M. F. Adams, J. Brown, P. Brune, K. Buschelman, V. Eijkhout, W. D. Gropp, D. Kaushik, M. G. Knepley, L. Curfman McInnes, K. Rupp, B. F. Smith, H. Zhang, *PETSc User Manual*, Argonne National Laboratory ANL-95/11 - Revision 3.4 (2013)
- [3] S. Balay, W. D. Gropp, L. Curfman McInnes, B. F. Smith, *Efficient Management of Parallelism in Object Oriented Numerical Software Libraries*, Modern Software Tools in Scientific Computing, Editors E. Arge, A. M. Bruaset and H. P. Langtangen (1997) Birkhä user Press.
- [4] Banaś, K. and Plaszcwski, P. and Maciol, P., Numerical integration on GPUs for higher order finite elements, *Computers and mathematics with applications* (2014) 67(6) 1319-1344.
- [5] Banas, K., Scalability analysis for a multigrid linear equations solver, *Lecture Notes in Computer Science* (2008) 4967, 1265-1274
- [6] N. Collier, L. Dalcin, V. M. Calo., *PetIGA: High-performance isogeometric analysis*, arxiv, (1305.4452), (2013) <http://arxiv.org/abs/1305.4452>

- [7] J. A. Cottrell, T. J. R. Hughes, Y. Bazilevs, *Isogeometric Analysis: Toward Unification of CAD and FEA* John Wiley and Sons, (2009)
- [8] C. M. Elliott, H. Garcke, *On the Cahn-Hilliard equation with degenerate mobility* SIAM Journal of Mathematical Analysis, 27 (1996) 404-423.
- [9] H. Gomes, V. M. Calo, Y. Bazilevs, T.J.R. Hughes, *Isogeometric analysis of the Cahn-Hilliard phase-field model*, Computer Methods in Applied Mechanics and Engineering, 197 (2008) 4333-4352.
- [10] Kruzel, F. and Banaś, K., Vectorized OpenCL implementation of numerical integration for higher order finite elements, *Computers and mathematics with applications* (2013) 66(10) 2030-2044.
- [11] K. Kuznik, M. Paszynski, V. Calo, Graph grammar based multi-frontal solver for isogeometric analysis in 1D, *Computer Science*, 14(4) (2013), 589-613
- [12] S.M. Wise, J.S. Lowengrub, H.B. Frieboes, V. Cristini, Three-Dimensional Diffuse-Interface Simulation of Multispecies Tumor Growth: Numerical Method, *Journal of Theoretical Biology*, 253(3) (2008) 524-43.
- [13] M. Woźniak, K. Kuźnik, M. Paszyński, V. M. Calo, D. Pardo, *Computational cost estimates for parallel shared memory isogeometric multi-frontal solvers*, *Computers and Mathematics with Applications*, 67(10) (2014) 1864-1883.
- [14] M. Woźniak, M. Paszyński, D. Pardo, L. Dalcin, V. M. Calo, *Computational cost of isogeometric multi-frontal solvers on parallel distributed memory machines*, *Computers and Mathematics with Applications* (2014) doi:10.1016/j.cma.2014.11.020
- [15] Woźniak, M., Fast GPU integration algorithm for isogeometric finite element method solvers using task dependency graphs, *Journal of Computational Science*, (2015) in press. corrected proofs, doi:10.1016/j.jocs.2015.02.007
- [16] Schaefer, R. and Sędziwy, S., *Filtration in cohesive soils. Part II - Numerical approach*, *Computer Assisted Mechanics and Engineering Sciences (CAMES)*, 6, (1999) 15-26.
- [17] Zlámal, M., *Finite element methods in heat conduction problems*, Proc. of the Conf. "The mathematics of finite elements and applications", Academic Press (1975).